

On the Kinematics of a Double-Cone Gravitational Motor

Barenten Suci

Department of Intelligent Mechanical Engineering, Fukuoka Institute of Technology, Fukuoka, 811-0295 Japan
(suci@fit.ac.jp)

Abstract-Kinematics of a double-cone self-propelled on a straight V-shape horizontal rail is investigated. This mechanism can be regarded as a gravitational motor that transforms the potential energy into kinetic energy, of rotation and translation. Movies of carbon steel double-cones rolling on aluminum rails were shot for various opening angles of the rails. Variable period of rotation, the number of rotations, and the total traveling time of the double-cone are obtained through slow motion processing of the taken movies. Proposed theoretical model, which is quite well validated by the experimental results, proves that the point of contact moves on the conical surface along a logarithmic spiral. Results obtained in this work are useful for the proper design of such gravitational motor.

Keywords-Double-cone, Point of contact, Logarithmic spiral, Gravitational motor, Kinematics

I. INTRODUCTION

First mention in the recorded history of a double-cone, able to self-propel due to the action of gravity along straight rails, upwardly directed and disposed as a V letter, i.e., the so-called “ascending cone” [1, 2], is related to Leonardo da Vinci from the European Renaissance period in the 15 century. Later, in 1829, the idea of a self-moving train using such gravitational motor that transforms the potential energy into kinetic energy of rotation and translation, was patented, but not turned into practice. Although, the apparent paradox of the ascending cone is a subject treated by the introductory Physics in connection to the center of mass (gravity), still there are several mechanical aspects, insufficiently explained. In order to clarify the basic educational aspects of the problem, accessible Physics tests to be performed in class, and simplified theoretical models were proposed [1]. On the other hand, sophisticated models, both from the physical and mathematical standpoints, of the rolling friction in general [3], and of the ascending cone problem in particular [2], can be found in the literature.

Although the gravitational motors employing double-cones have relative large applicative potential, the concrete range of practical applications remains unsettled. One of the reasons is that, in order to properly design such mechanism, a relatively simple theoretical model, but sufficiently well validated by the experimental results is needed. To achieve such target, in this work, firstly movies of carbon steel double-cones, rolling on straight V-shape horizontally displaced aluminum rails, were shot for various opening angles of the rails. Then, through slow

motion processing of the taken movies, the variable period of rotation, the number of rotations, and the total traveling time of the double-cone are obtained. Next, a theoretical model, which is relatively well validated by the experimental results, is proposed. Based on such geometrical and kinematical analysis, one proves that the points of contact between the double-cone and rails move on the conical surface along a logarithmic spiral.

II. TEST RIG AND EXPERIMENTAL PROCEDURE

Two cones made of S45C carbon steel, each having a height H and a radius R at the base circle, are joined together by using a bonding adhesive, to achieve a double-cone (Fig. 1). In order to experimentally observe the influence of the apex angle $\Psi = \tan^{-1}(R/H)$ of the cone, two types of double-cones having different dimensions, were manufactured. Thus, Table I shows the physical (diameter $2R$ at the base circle, total height $2H$, apex angle, mass m , and moment of inertia $I = 0.3mR^2$), material (modulus of elasticity E_c , and Poisson's ratio ν_c) and tribological (static friction coefficient μ_s and dynamic friction coefficient μ against the aluminum rails) properties of the tested double-cones. Aluminum rails having the modulus of elasticity of $E_r = 74\text{GPa}$, the Poisson's ratio of $\nu_r = 0.33$, the length of $L_0 = 1,000$ m, the height of $H_0 = 50$ mm, and the chamfering radius of $R_0 = 1$ mm, are disposed on a horizontal table forming a V letter of entrance L_2 and exit L_1 (Figs. 2-8).

Double-cone made of S45C carbon steel,
 $m = 1.05$ kg; $R = 25$ mm; $H = 100$ mm



Double-cone made
of S45C steel,
 $m = 0.63$ kg;
 $R = 27.5$ mm;
 $H = 48$ mm

Figure 1. Photographs and physical properties of the tested double-cones.

TABLE I. PHYSICAL, MATERIAL AND TRIBOLOGICAL PROPERTIES OF THE TESTED DOUBLE-CONES [4-6]

Property	Double-cone 1	Double-cone 2
Diameter, $2R$ [mm]	50	55
Total height (length), $2H$ [mm]	200	96
Mass, m [kg]	1.05	0.63
Moment of inertia, I [$\text{kg}\cdot\text{mm}^2$]	197	143
Apex angle, Ψ [deg]	14.036	29.809
Material	S45C steel	S45C steel
Modulus of elasticity, E_c [GPa]	206	206
Poisson's ratio, ν_c [-]	0.3	0.3
Static friction coefficient, μ_s [-]	0.61	0.61
Dynamic friction coefficient, μ [-]	0.47	0.47
Entrance distance of rails, L_2 [mm]	0, 10, ..., 180	0, 10, ..., 90
Exit distance of rails, L_1 [mm]	185	90

Fig. 2 shows the geometry of the employed double-cone and V-shape rails. Exit distance of the rails is set to a constant value of $L_1 = 185$ mm in the case of double-cone 1, and $L_1 = 90$ mm in the case of double-cone 2 (Table I). On the other hand, the entrance distance L_2 of the rails is taken as variable, i.e., it is adjusted with a pitch of 10 mm, from 0 to 180 mm in the case of double-cone 1, and from 0 to 90 mm in the case of double-cone 2. For instance, Fig. 3 shows photographs of the rolling double-cone 1 for two values of the entrance distance of $L_2 = 0$ and 180 mm.

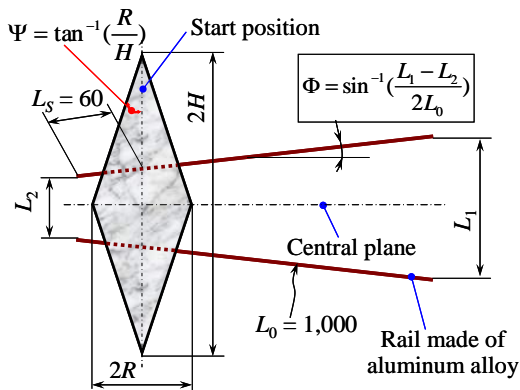


Figure 2. Geometry of the double-cone and V-shape rails.

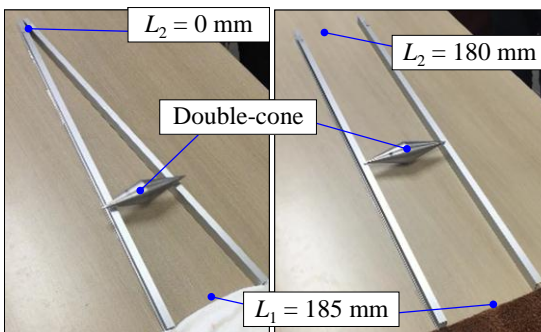


Figure 3. Photographs of the rolling double-cone 1 for $L_2 = 0$ and 180 mm entrance distances.

Note that for $L_2 = L_1$, rails become parallel and in such case the double-cone is unable to self-propel along the rails. In fact, as it will be discussed later in detail, the double-cone 2 is unable to self-propel if $L_2 \geq 80$ mm. In order to quantify the influence of the entrance distance on the obtained experimental results, the opening angle of the rails is defined as (Fig. 2):

$$\Phi = \sin^{-1}\left(\frac{L_1 - L_2}{2L_0}\right) \quad (1)$$

Angle Φ linearly decreases from its maximal value obtained for $L_2 = 0$, which is of 5.307 deg for double-cone 1, and of 2.579 deg for double-cone 2, to its minimal value of 0 deg obtained for parallel tracks (see Fig. 4).

In order to achieve good repeatability of the experimental results, the start point of the rolling tests is taken in such a way that the axis of the double-cone is always placed at a distance $L_S = 60$ mm, measured from the entrance point along the rails (Fig. 2). On the other hand, rolling tests can be conducted only if the following geometrical conditions are fulfilled (Figs. 2-8):

$$L_2 \leq L_1 \quad ; \quad L_1 \leq 2H \quad ; \quad R \leq H_0 \quad (2)$$

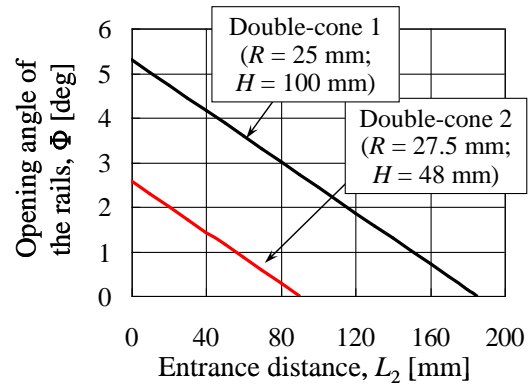


Figure 4. Variation of the opening angle versus the entrance distance.

The experimental procedure can be summarized as follows:

- 1) Aluminum rails, with a height larger than the radius of the double-cone ($H_0 \geq R$), are placed on a horizontal table in such a way that a V letter is formed. Exit distance is fixed to a desired value, which has to satisfy the condition: $L_1 \leq 2H$.
- 2) Variable entrance distance of the rails is adjusted to a desired value, which has to satisfy the condition: $L_2 \leq L_1$.
- 3) Double-cone is carefully placed on the rails at the start position ($L_S = 60$ mm, in Fig. 2), to avoid supplying of input kinetic energy into the system.
- 4) Double-cone starts to self-propel along the rails due to the gained initial potential energy, which is transformed into kinetic energy, of rotation and translation (Fig. 12). However, for entrance distances close to the exit distance ($L_2 \approx L_1$), the double-cone is unable to self-propel along the rails.
- 5) In order to easily observe the movement of the double-cone along the rails, cone generatrix and circular symbols were

drawn (Fig. 1). For various opening angles of the rails, movies were shot from a convenient position near the exit of the tracks. In the same time, the total travelling time T of the double-cone was measured by using a stop-watch (see Table II). In order to improve the accuracy of the experimental results, for each selected opening angle, 3 tests were performed, and the mean values were calculated.

6) Through slow motion processing of the taken movies the variable period of rotation T_i ($i = 1 - n$) and the number of rotations n were determined. Summation of all these periods of rotation provided also for an estimation of the total traveling time of the double-cone $T_m = \sum_{i=1}^n T_i$ (Table II). Results obtained by using the stop-watch and the slow motion processing of the movies are in quite good agreement (see Table II).

III. EXPERIMENTAL RESULTS

Table II presents the variation of the number of rotations n , the total traveling time T measured by using a stop-watch, and the total traveling time T_m calculated from the recorded movies of the double-cones 1 and 2, rolling on V-shape horizontal rails.

One observes that at augmentation of the entrance distance the total traveling time and the number of rotations of the double-cone increases. Since the relative difference of the total traveling time, measured by stop-watch and also determined through the slow motion processing of the movies, is smaller than 10%, one concludes that the travelling time of the double-cone was estimated quite precisely.

TABLE II. VARIATION OF THE NUMBER OF ROTATIONS, TOTAL TRAVELING TIME MEASURED BY USING A STOP-WATCH, AND THE TOTAL TRAVELING TIME CALCULATED FROM THE RECORDED MOVIES

Entrance distance L_2 [mm]	Double-cone 1			Double-cone 2		
	n [-]	T [s]	T_m [s]	n [-]	T [s]	T_m [s]
0	16.5	3.94	3.906	17.0	4.09	4.124
10	17.0	4.27	4.132	17.5	4.72	4.468
20	18.2	4.49	4.422	19.0	5.26	5.084
30	18.5	4.66	4.442	20.0	5.93	5.886
40	20.0	4.93	4.936	22.0	7.13	7.032
50	20.5	5.20	5.096	27.0	9.08	8.810
60	21.0	5.51	5.340	30.0	11.97	11.492
70	22.0	5.90	5.810	36.0	18.77	18.010
80	23.0	6.30	6.280	---	---	---
90	24.0	6.91	6.748	---	---	---
100	25.5	7.48	7.340	---	---	---
110	27.5	8.48	8.302	---	---	---
120	29.3	9.45	9.380	---	---	---
130	31.7	10.82	10.578	---	---	---
140	34.2	12.98	12.866	---	---	---
150	38.0	16.30	15.882	---	---	---
160	42.5	19.99	19.476	---	---	---
170	49.0	25.92	26.200	---	---	---
180	58.0	34.65	38.546	---	---	---

IV. THEORETICAL MODEL

Friction forces, acting in the contact points P and Q during the movement of the double-cone on the rails (Fig. 6), are vectors occurring along rails, opposing the advance direction of the double-cone (Fig. 5):

$$\begin{cases} \vec{F}_{f,P} = -N_P \mu (\cos \Phi \vec{i} + \sin \Phi \vec{j}) \\ \vec{F}_{f,Q} = -N_Q \mu (\cos \Phi \vec{i} - \sin \Phi \vec{j}) \end{cases} \quad (3)$$

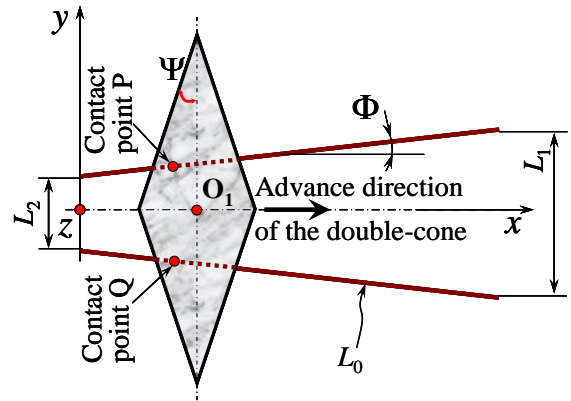


Figure 5. Upper view of the contact between the double-cone and rails.

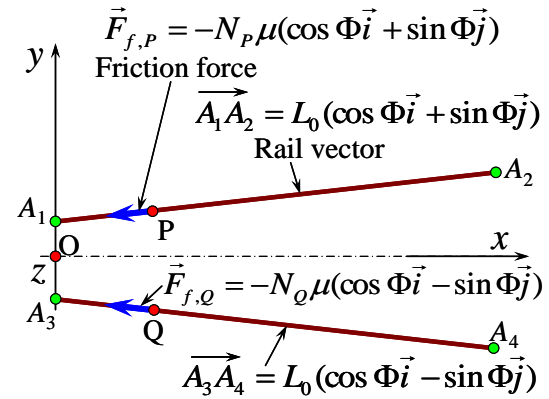


Figure 6. Definition of the rail vectors and friction forces.

Here N_P and N_Q are the moduli of the reaction forces acting in the contact points P and Q, which can be written as (Figs. 7, 8):

$$\begin{cases} \vec{N}_P = N (\cos \Psi \sin \alpha_1 \vec{i} - \sin \Psi \vec{j} + \cos \Psi \cos \alpha_1 \vec{k}) \\ \vec{N}_Q = N (\cos \Psi \sin \alpha_1 \vec{i} + \sin \Psi \vec{j} + \cos \Psi \cos \alpha_1 \vec{k}) \end{cases} \quad (4)$$

Due to the geometrical symmetry of the mechanism relative to the Ox axis (Fig. 5), the reaction forces acting in the contact points P and Q should have the same moduli, as follows:

$$N_P = N_Q = N \sqrt{\cos^2 \Psi (\sin^2 \alpha_1 + \cos^2 \alpha_1) + \sin^2 \Psi} = N \quad (5)$$

Note that, on one hand, in the contact points P and Q, the friction forces should be normal on the reaction forces. Thus, the scalar product of the vectors describing the friction forces and the reaction forces should be nil:

$$\begin{cases} \vec{N}_P \perp \vec{F}_{f,P} \\ \vec{N}_Q \perp \vec{F}_{f,Q} \end{cases} \Rightarrow \begin{cases} \vec{N}_P \cdot \vec{F}_{f,P} = 0 \\ \vec{N}_Q \cdot \vec{F}_{f,Q} = 0 \end{cases} \quad (6)$$

Condition (6) leads to the following relationship for the angle α_1 defined in Fig. 8:

$$\sin \alpha_1 = \tan \Phi \cdot \tan \Psi \quad (7)$$

Result (7) agrees with the previously reported findings [2].

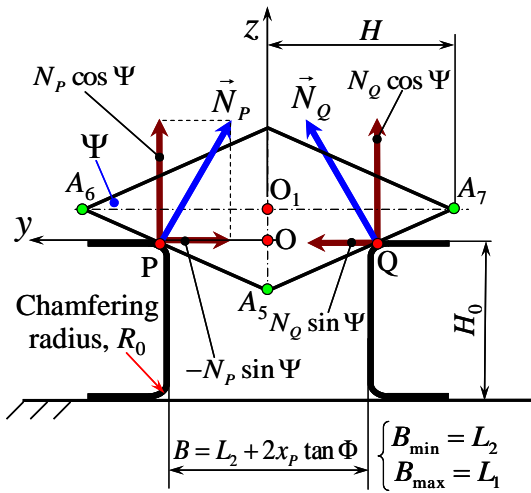


Figure 7. Frontal view of the contact between the double-cone and rails.

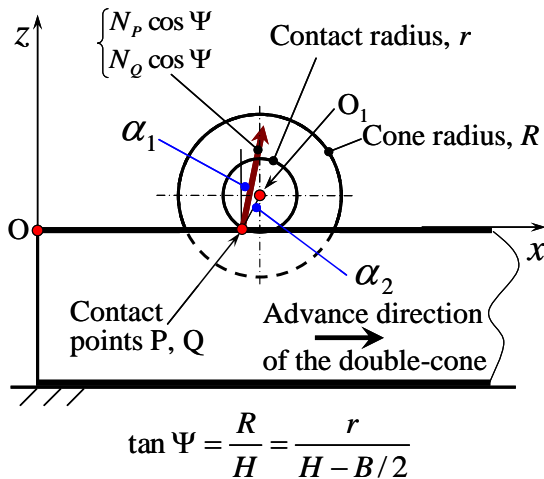


Figure 8. Lateral view of the contact between the double-cone and rails.

In order to find the relationship between the angles α_1 and α_2 (Fig. 8), one firstly searches for the coordinates corresponding to the contact points P and Q, for the bottom point A_5 , as well as for the end points A_6 and A_7 of the double-cone (Fig. 7):

$$P(x_p, B/2, 0) ; Q(x_p, -B/2, 0) \quad (8)$$

$$\begin{cases} A_5(x_p + (r-R) \sin \alpha_2, 0, (r-R) \cos \alpha_2) \\ A_6(x_p + r \sin \alpha_2, H, r \cos \alpha_2) \\ A_7(x_p + r \sin \alpha_2, -H, r \cos \alpha_2) \end{cases} \quad (8')$$

Thus, the generatrix containing the contact points can be written as full vectors (Fig. 9):

$$\begin{cases} \vec{A_5A_6} = R(\sin \alpha_2 \vec{i} + \cot \Psi \vec{j} + \cos \alpha_2 \vec{k}) \\ \vec{A_5A_7} = R(\sin \alpha_2 \vec{i} - \cot \Psi \vec{j} + \cos \alpha_2 \vec{k}) \end{cases} \quad (9)$$

or as partial vectors, as follows:

$$\begin{cases} \vec{PA_6} = r(\sin \alpha_2 \vec{i} + \cot \Psi \vec{j} + \cos \alpha_2 \vec{k}) \\ \vec{QA_7} = r(\sin \alpha_2 \vec{i} - \cot \Psi \vec{j} + \cos \alpha_2 \vec{k}) \end{cases} \quad (9')$$

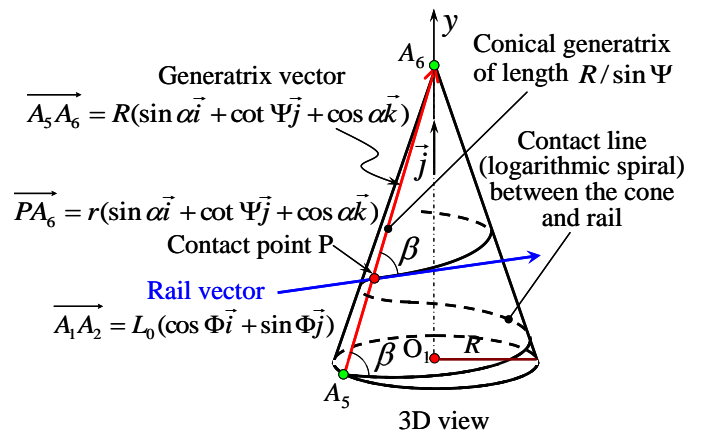


Figure 9. 3D view of the contact line between the conical surface and the rail.

Note that, on the other hand, in the contact points P and Q, the reaction forces should be normal on the generatrix vectors. Thus, the scalar product of the vectors describing the reaction force and the generatrix should be nil:

$$\begin{cases} \vec{N}_P \perp \vec{PA_6} \\ \vec{N}_Q \perp \vec{QA_7} \end{cases} \Rightarrow \begin{cases} \vec{N}_P \cdot \vec{PA_6} = 0 \\ \vec{N}_Q \cdot \vec{QA_7} = 0 \end{cases} \quad (10)$$

Condition (10) leads to the following relationship between the angles α_1 and α_2 defined in Fig. 8:

$$\cos \Psi (\sin \alpha_1 \sin \alpha_2 - 1 + \cos \alpha_1 \cos \alpha_2) = 0 \quad (11)$$

Note that (11) finally reduces to the equality of these angles. For this reason, the subscript can be disregarded, as follows:

$$\cos(\alpha_1 - \alpha_2) = 1 \Rightarrow \alpha_1 = \alpha_2 = \alpha \quad (12)$$

Next, one proves that points P and Q of the contact between the double-cone and rails move on the conical surface along a three-dimensional (3D) curvilinear trajectory, which is in fact a 3D logarithmic spiral (see Fig. 9). This can be demonstrated under the assumption that the double-cone has a pure rolling movement along the rails, i.e., there is no slip at the contact

points P and Q between the double-cone and the rails. In such circumstances, the distance traveled by the contact point P on the straight rail equals the distance traveled by the same contact point P along the curved arch of the 3D curvilinear trajectory.

With this purpose, one evaluates the angle β between the generatrix containing the contact point and the corresponding rail. Concretely, from the scalar product of the generatrix and rail vectors:

$$\cos \beta = \frac{\vec{A_1A_2} \cdot \vec{A_5A_6}}{A_1A_2 \cdot A_5A_6} \quad (13)$$

the following relationship for the angle β can be found:

$$\cos \beta = (\sin \alpha \cos \Phi + \cot \Psi \sin \Phi) \sin \Psi = \frac{\sin \Phi}{\cos \Psi} \quad (14)$$

Since angle β according to (14) is depending only on the apex angle Ψ of the double-cone and the opening angle Φ of the rails, for a given geometry of the gravitational motor, angle β appears as constant. Further, it linearly increases from its minimal value obtained for $L_2 = 0$, which is of 84.529 deg for double-cone 1, and of 87.027 deg for double-cone 2, to its maximal value of 90 deg obtained for parallel tracks (Fig. 10).

Based on this particularity of the angle β one proves, as follows, that the contact point moves on the conical surface along a path, which is logarithmic spiral [7]. With this purpose, first, the 3D conical surface shown in Fig. 9 is developed as a circular sector with a radius of $R/\sin \Psi$ and an opening angle of $\gamma = 2\pi \sin \Psi$ in the plane described by the polar coordinates (ρ, θ) (Fig. 11). In this plane, the curvilinear contact line can be described by the following differential equation [7]:

$$\frac{d\rho}{\rho} = -\frac{1}{\tan \beta} d\theta \quad (15)$$

Then, (15) is integrated for all curvilinear paths corresponding to rotations of the double-cone from 1 to n , as follows:

$$\rho = \frac{R}{\sin \Psi} \exp\left[-\frac{\theta}{\tan \beta} - 2\pi(i-1) \tan \alpha\right] ; \quad i = \overline{1, n} \quad (16)$$

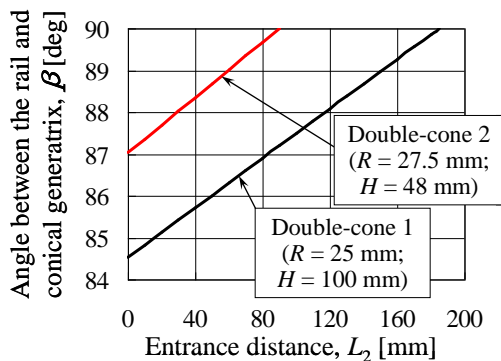


Figure 10. Variation of the angle measured between the rail and the conical generatrix containing the contact point versus the entrance distance.

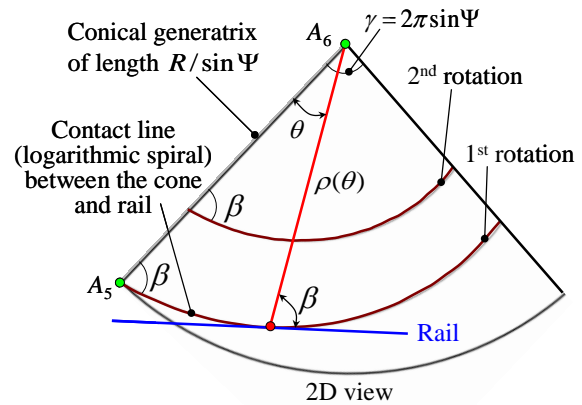


Figure 11. 2D view of the contact line between the conical surface and the rail.

Thus, (16) shows that indeed the contact line is described by a logarithmic spiral. Next, rewriting (14) as follows:

$$\tan \beta = \frac{\cos \Psi \cos \alpha}{\tan \Phi} \quad (17)$$

and imposing the previously argued condition, i.e., the distance traveled by the contact point P on the straight rail equals the distance traveled by the same contact point P along the curved arch of the curvilinear trajectory, one obtains the theoretical number of rotations n_i of the double-cone, as follows:

$$n_i = -\frac{1}{2\pi \tan \alpha} \ln\left(1 - \frac{L_0 - L_s}{r_0} \sin \Phi \tan \Psi\right) \quad (18)$$

Here $L_0 - L_s$ is the distance travelled by the contact point along the rail, and r_0 is the contact radius at the start position of the double-cone (see Figs. 2 and 12). In order to determine the start contact radius, one firstly observes the relationship between the coordinates of the contact point P and the center O_1 of the double-cone, as follows:

$$\begin{cases} x_{O_1} = x_p + r \sin \alpha \\ y_p = 0.5L_2 + x_p \tan \Phi \quad (y_{O_1} = 0) \\ z_{O_1} = r \cos \alpha \quad (z_p = 0) \end{cases} \quad (19)$$

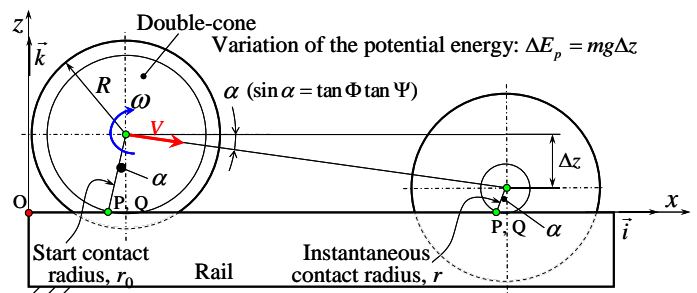


Figure 12. Change in the radius of contact and implicitly, change in the height of the mass center due to the movement of the double-cone on the rails.

Next, taking into account that the instantaneous contact radius satisfies the following equation (see Fig. 8):

$$\tan \Psi = \frac{R}{H} = \frac{r}{H - B/2} \quad (20)$$

where the instantaneous width of the rails is given by (Fig. 7):

$$B = L_2 + 2x_p \tan \Phi \quad (21)$$

one finds the following relationship for the contact radius:

$$r = R - 0.5L_2 \tan \Psi - x_p \sin \alpha \quad (22)$$

Then, by substituting the first equation of (19) into (22), the contact radius can be rewritten as:

$$r = \frac{R - 0.5L_2 \tan \Psi - x_{o_1} \sin \alpha}{\cos^2 \alpha} \quad (23)$$

Since at the start position, the longitudinal coordinate of the center O_1 of the double-cone is given by (see Fig. 2):

$$x_{o_1} = L_s \cos \Phi \quad (24)$$

the contact radius at the start position becomes:

$$r_0 = \frac{R}{\cos^2 \alpha} \left[1 - \frac{L_2}{2H} - \frac{(L_1 - L_2)L_s}{2HL_0} \right] \quad (25)$$

Substituting (25) in (18) one obtains the theoretical number of rotations n_t of the double-cone, as follows:

$$n_t = - \frac{\ln \left[1 - \frac{(L_0 - L_s)(L_1 - L_2) \cos^2 \alpha}{2HL_0 - L_2L_0 - (L_1 - L_2)L_s} \right]}{2\pi \tan \alpha} \quad (26)$$

V. RESULTS AND DISCUSSIONS

Fig. 13 illustrates the variation of the number of rotations versus the entrance distance, obtained from the experimental data and from the proposed theoretical model, for double-cones 1 and 2. Number of rotations nonlinearly increases against the entrance distance.

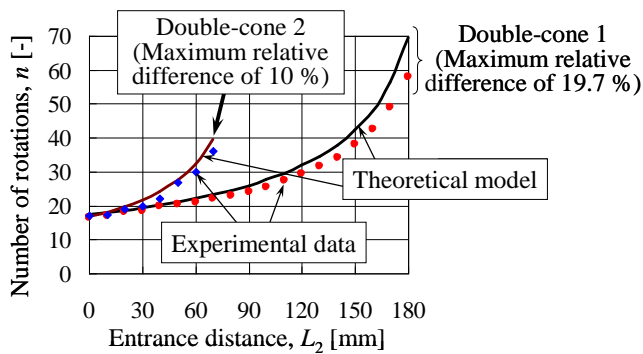


Figure 13. Variation of the number of rotations versus the entrance distance, obtained from the experimental data and from the proposed theoretical model, for double-cones 1 and 2.

Rate of augmentation is higher for the double-cone 2, which has larger apex angle.

Since the maximum relative difference is smaller than 10 % for the double-cone 2, and smaller than 19.7 % for the double-cone 1, one concludes that the results obtained by using the proposed model are in relatively good agreement with the experimental results, measured for double-cones made of carbon steel, rolling against aluminum rails. Again, proposed model is better validated by the experimental results obtained for the double-cone 2, which has larger apex angle.

Although the geometrical and kinematical model proposed in this work has somewhat limited accuracy, it might be used to design, at least in a first approximation, the gravitational motor. Observed differences between the theoretical predictions and the measured data might be induced by the influence of slippage at the contact points, and also by the influence of the friction, which were neglected. Improvement of the theoretical model by taking into account these effects will be considered in our future work.

Differentiating the third equation of (19) and also (23), one obtains:

$$\frac{dz_{o_1}}{dr} = \cos \alpha \quad ; \quad \frac{dr}{dx_{o_1}} = - \frac{\sin \alpha}{\cos^2 \alpha} \quad (27)$$

which leads to the following relationship between the axial and vertical coordinates of the center O_1 of the double-cone:

$$\frac{dz_{o_1}}{dx_{o_1}} = - \tan \alpha \quad (28)$$

This means that the center O_1 of the double-cone moves along a straight descending line, which displays a descending angle α relative to the horizontal direction (see Fig. 12). Result (28) agrees with the previously reported findings [2].

Thus, the gradual reduction of the contact radius leads to a proportional reduction in the height of the mass center Δz of the double-cone. This causes a proportional decrease of the potential energy $\Delta E_p = mg\Delta z$ of the double-cone, from the initial input potential energy (see Fig. 12). For this reason, such mechanism can be regarded as a gravitational motor, which transforms the potential energy into kinetic energy, of rotation and translation.

From a practical standpoint, maximization of the number of rotations of the gravitational motor can be required. In order to achieve this, one takes the exit distance L_1 of the rails at its maximal value, which equals the total height $2H$ of the double-cone ($2H = L_1$). In such circumstances, the angle α given by (7) and (12) reaches its maximal value, as follows:

$$\sin \alpha_{\max} = \frac{R}{H} \frac{2H - L_2}{\sqrt{4L_0^2 - (2H - L_2)^2}} \quad (29)$$

Additionally, the theoretical number of rotations of the double-cone given by (26) reaches its maximal value as described by the following expression:

$$n_{t,\max} = -\frac{\ln(\sin \alpha_{\max})}{\pi \tan \alpha_{\max}} \quad (30)$$

Fig. 14 illustrates the variation of the maximal number of rotations $n_{t,\max}$ versus the entrance distance, as predicted by the proposed theoretical model (29, 30), for double-cones 1 and 2. Similar to Fig. 13, number of rotations nonlinearly increases against the entrance distance, the rate of augmentation being higher for the double-cone 2, which has larger apex angle.

Comparison of the results shown by Fig. 13 and Fig. 14 proves that the number of rotations of the gravitational motor can be considerably increased through adequate selection of the geometrical parameters.

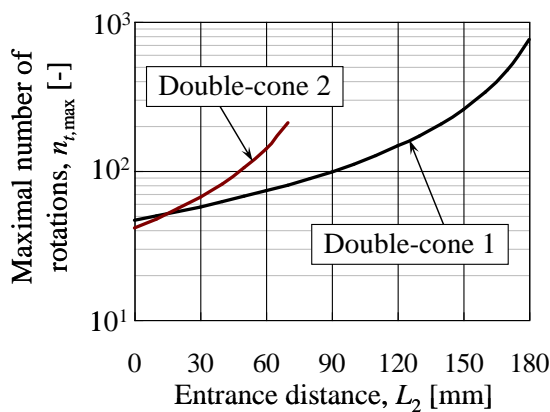


Figure 14. Variation of the maximum number of rotations versus the entrance distance, predicted by the proposed theoretical model, for double-cones 1 & 2.

VI. SUMMARY

In this work, the kinematics of a double-cone self-propelled on a straight V-shape horizontal rail was investigated. This mechanism was treated as a gravitational motor able to change the input potential energy into kinetic energy, of rotation and translation. Movies of carbon steel double-cones rolling on aluminum rails were shot for various opening angles of the

rails. Variable period of rotation, the number of rotations, and the total traveling time of the double-cone were obtained through the slow motion processing of the taken movies. A theoretical model was proposed and validated by the experimental results. One proved that the point of contact moves on the conical surface along a logarithmic spiral. Although the kinematical model has somewhat limited accuracy, it might be used to design, at least in a first approximation, the gravitational motor. If required from a practical standpoint, maximization of the number of rotations of the gravitational motor can be achieved, based on the model proposed.

REFERENCES

- [1] A. A. Gallitto, and E. Fiordilino, "The double cone: a mechanical paradox or a geometrical constraint?," *Physics Education*, vol. 46, pp. 682–684, 2011.
- [2] S.C. Gandhi, and C.J. Efthimiou, "The ascending double-cone a closer look at a familiar demonstration," *European Journal of Physics*, vol. 26, pp. 681–697, 2005.
- [3] A. Domenech, T. Domenech, and J. Cebrian, "Introduction to the study of rolling friction," *American Journal of Physics*, vol. 55, no. 3, pp. 231–235, 1987.
- [4] U. Olofsson, and R. Lewis, *Tribology of the Wheel-Rail Contact*, Taylor & Francis, pp. 121–141, 2012.
- [5] G.W. Stachowiak, and A.W. Batchelor, *Engineering Tribology*, 3rd Edition, Elsevier, pp. 287–362, 461–499, 2005.
- [6] A. Kapoor, D.I. Fletcher, F. Schmid, K.J. Sawley, and M. Ishida, *Tribology of Rail Transport*, CRC Press, pp. 161–202, 2001.
- [7] Y. Ye, and J. Zhu, "Geometric studies on variable radius spiral cone-beam scanning," *Medical Physics*, vol. 31, no. 6, pp. 1473–1480, 2004.



Barenten Suciu was born on July 9, 1967. He received Dr. Engineer Degrees in the field of Mechanical Engineering from the Polytechnic University of Bucharest, in 1997, and from the Kobe University, in 2003. He is working as Professor at the Department of Intelligent Mechanical Engineering, Fukuoka Institute of Technology. He is also entrusted with the function of Director of the Electronics Research Institute, affiliated to the Fukuoka Institute of Technology. He is member of JSME and JSAE. His major field of study is the tribological and dynamical design of various machine elements.